*Tellus (1997), 49A, 87–99*
*Printed in UK – all rights reserved*

*Copyright © Munksgaard, 1997*
**TELLUS**
*ISSN 0280–6495*

# On the modification of the high- and low-frequency eddies associated with the PNA anomaly: an observational study

By HAI LIN* and JACQUES DEROME, *Department of Atmospheric and Oceanic Sciences and Centre for Climate and Global Change Research, McGill University, 805 Sherbrooke Street West, Montréal, Québec H3A 2K6, Canada*

(Manuscript received 24 July 1995; in final form 12 April 1996)

ABSTRACT

A 24-year NMC data set was used to study the interannual fluctuations in the extratropical atmospheric flow and the interactions between transients of different frequencies. Significant differences were found in the transient activities between winters with positive and negative Pacific/North American (PNA) seasonal anomalies. During the winters with an enhanced positive PNA pattern, the eddy activity is reduced over the North Pacific. The reduction of eddy activity is dominated by the low-frequency transients (periods from 10 days to a season). The occurrence of persistent anomalies in this region is also less frequent. The high-frequency baroclinic waves are shifted south-eastward of their normal position in the Pacific. The weak low-frequency activity over the North Pacific during positive PNA winters is linked to two processes. Firstly, the large-scale seasonal mean flow makes a smaller contribution to the low-frequency height variance. Secondly, the strong seasonal-mean Aleutian low tends to keep the baroclinic synoptic-scale eddies moving along its southern side, causing only a weak interaction with the low-frequency eddies over the North Pacific, and thus a smaller synoptic-scale eddy forcing of the low-frequency flow. The low-frequency activity is closely associated with the atmospheric natural variability which causes error growth in medium- and extended-range numerical predictions. Our result suggests that during positive PNA winters a better predictive skill for medium- and extended-range numerical predictions may be possible.

## 1. Introduction

Considerable variability in predictive skill has been observed in medium- to long-range weather predictions (Mansfield, 1986; Miyakoda et al., 1986). It would be of considerable practical interest to know how the predictive skill depends on the type of weather regime for which a prediction is being made.

Branstator et al. (1993) and Renwick and Wallace (1995) have found that the most predictable anomaly pattern in the atmosphere is the leading EOF of the wintertime 500 hPa height field, which has a structure similar to the Pacific/North American (PNA) pattern. It is also found that the polarity of this pattern is particularly well predicted, and its amplitude is forecast with approximately equal skill in either polarity.

It is noted that in the studies of Branstator et al. (1993) and Renwick and Wallace (1995) analyses were made on forecasts up to 10 days. The predicted anomaly patterns have rather short time scales and are associated with natural variabilities that are generated by the internal dynamics of the atmosphere. The error growth on such time scales is strongly dependent on the intensity of the natural variability. In this study we are interested in how the intensity of the natural variability is linked to the background flow pattern and its

* Corresponding author. Email: hlin@zephyr.meteo.mcgill.ca

interannual variations, as a possible step to understanding the interannual variations of the forecast skill.

In a recent study, Chen and Van Den Dool (1995) (hereafter CV) examined the low-frequency variability with time-scales between 7 and 31 days in different basic flows over the North Pacific. They found that there is much smaller variability for North Pacific cyclonic basic flows than anticyclonic basic flows, and they implied that the potential predictability of monthly means would be higher in the North Pacific cyclonic basic flows.

In the present study we compare the intraseasonal fluctuations with time scales from 10 days to 90 days during winters with positive and negative PNA anomalies. In doing so we hope to obtain some useful information on a possible relation between the predictability of the atmosphere and the background PNA weather regime. We study how the extratropical low-frequency transients differ between positive and negative PNA anomalies in the background seasonal mean flow. The mechanisms behind the difference of the low-frequency eddy activity are analyzed by means of the tendency equation for the low-frequency height variance. The feedbacks to the seasonal mean flow from both the intraseasonal eddies and the synoptic-scale transients are also discussed.

This study is related to that of CV, but differs in a number of ways. In defining the anomalous basic flow, CV used one representative point in the North Pacific, while we use the PNA index of the wintertime seasonal mean. The time series of these two parameters, however, are strongly correlated. The PNA pattern represents the leading EOF of the wintertime seasonal mean 500 hPa height (Wallace et al., 1993). Our definition is less localized than CV's and represents the most significant wintertime anomaly pattern over the Northern Hemisphere. A second difference is that we study the interactions among three frequency bands, i.e., the seasonal mean, the low-frequency and high-frequency (synoptic-scale) flows, while CV did not consider the interactions between low- and high-frequencies. Thus we are able to provide additional information on the atmospheric internal dynamic processes and their differences in positive and negative PNA regimes. In discussing the weak low-frequency variability in the North Pacific cyclonic basic flows, CV showed that it is associated with a weak kinetic energy conversion from the basic mean flow. We will use an equation for the low-frequency height variance to investigate the contributions from different processes. We will show that the anomalously weak synoptic-scale forcing also makes a significant contribution. The lengths of datasets used in these two studies are also different. We use data for 24 winters, while CV analyzed 8 winters.

The dataset used in this study is described in Section 2. Composite analyses for the winters with positive and negative PNA anomalies are documented in Section 3 to demonstrate the interannual variations in the seasonal mean flow and the transient activities. In Section 4, the interactions of the low-frequency transients with the seasonal mean flow and with the high-frequency eddies are discussed. The effects of the high- and low-frequency transients on the seasonal mean flow are discussed in Section 5. Finally a summary and discussion are given in Section 6.

## 2. The dataset

The data employed in this study are the twice-daily (0000 and 1200 GMT) analyses produced by the US National Meteorological Center (NMC). The variables that are available include the geopotential height at 850, 700, 500, and 200 hPa, and the wind at 850 and 250 hPa. The data were converted from an octagonal grid to a longitude-latitude grid extending from 20°N to the North Pole with a resolution of 5° in both longitude and latitude. Data for 24 winters from 1965/66 to 1988/89 are used. Winter is defined to be the 90 day period beginning at 0000 GMT 1 December. The geopotential height data cover all the 24 winters. The 850 hPa wind data for the 1965/66 and 1969/70 winters and the 250 hPa wind data for the 1969/70 winter are not available. Temporal data gaps within individual winters were filled using linear interpolation in time.

A transient is defined as the departure of the data from the seasonal mean. In order to separate the low-frequency eddies and the synoptic-scale transients, the Fourier filters used by Lin and Derome (1996) are applied to the twice-daily time series of data for each winter. The synoptic-scale transients are taken to be those with a frequency range corresponding to periods between 2 and 10

days, while the low-frequency eddies are those with periods from 10 to 90 days.

## 3. The interannual variations

The PNA pattern describes one of the most significant teleconnections in the atmosphere (Wallace and Gutzler, 1981), and represents the leading EOF of wintertime seasonal mean 500 hPa height (Wallace et al., 1993). In this study we will investigate the dependence of the atmospheric sub-seasonal natural variability on the polarity of the PNA circulation pattern.

One way to describe the variability of the PNA pattern is to use the PNA index. The index is calculated here for the seasonal mean flow (90 day average), and is defined following Wallace and Gutzler (1981) as

$$\text{PNA index} = \frac{1}{4}\,[z^*(20°\text{N}, 160°\text{W}) - z^*(45°\text{N}, 165°\text{W}) + z^*(55°\text{N}, 115°\text{W}) - z^*(30°\text{N}, 85°\text{W})], \quad (1)$$

where $z^*$ represents a departure of a particular winter season (90 days) from the wintertime climatological mean 500 hPa height for that grid point, normalized by the local standard deviation of that departure. The positive (negative) PNA index is associated with negative (positive) height anomalies over the North Pacific and Florida and positive (negative) height anomalies over Hawaii and northwest Canada.

The time series for the PNA index over the 24 winters is shown in Fig. 1. The years shown on the diagram refer to the beginning year of the winter season, i.e., 65 refers to the 1965/66 winter. To demonstrate the difference of the atmospheric states between the winters with positive and negative PNA indices, separate composites are made for the winters with extreme positive and negative PNA indices. The winters chosen for the composites are those with the PNA indices larger than $+0.5$ and those smaller than $-0.5$, that are marked by small circles and triangles in Fig. 1. We will refer to those winters with a PNA index $> +0.5$ and $< -0.5$ as those with positive and negative PNA anomalies, respectively. There are 7 winters with a positive PNA anomaly and 8 winters with a negative PNA anomaly according to this criterion. Of the positive PNA winters, 4 of them correspond to major El Niño events in the 24 years: 69/70, 76/77, 82/83 and 86/87. A student $t$–test method is used to analyze the significance of the difference between the two groups. Throughout this study the discussion is mainly focused on the circulation in the North Pacific area.

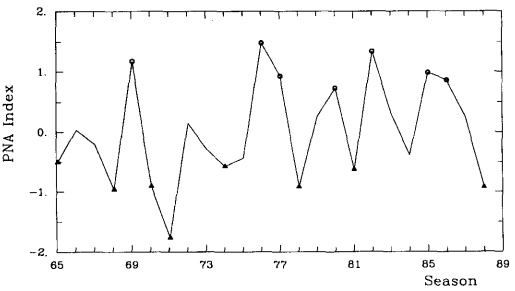


*Fig. 1.* Time series of PNA index. Points with small circles and triangles represent those selected as positive and negative PNA cases, respectively.

### 3.1. *The seasonal mean anomaly*

To give a reference of the PNA pattern for the rest of this study, Fig. 2 shows the 500 hPa geopotential height difference between winters of positive and negative PNA anomalies, as is obtained by subtracting the composite of the $-$PNA winters from that of the $+$PNA winters. The shaded areas are those with significance levels greater than 99% from the $t$–test.

Corresponding to the negative height anomaly in the North Pacific during winters with $+$PNA anomaly, the north-south pressure gradient in the central-eastern Pacific is anomalously large, as are the westerlies near 30°N. This phenomenon can also be viewed as the eastward extension of the westerly jet which normally appears over and east of Japan. In the 250 hPa zonal wind difference between the winters of positive and negative PNA anomalies (not shown), a positive anomaly near 30°N in the central-eastern Pacific is clear with a maximum in excess of 20 m/s.

### 3.2. *The transient activities*

The difference in the synoptic-scale transient rms of the 500 hPa geopotential height is shown

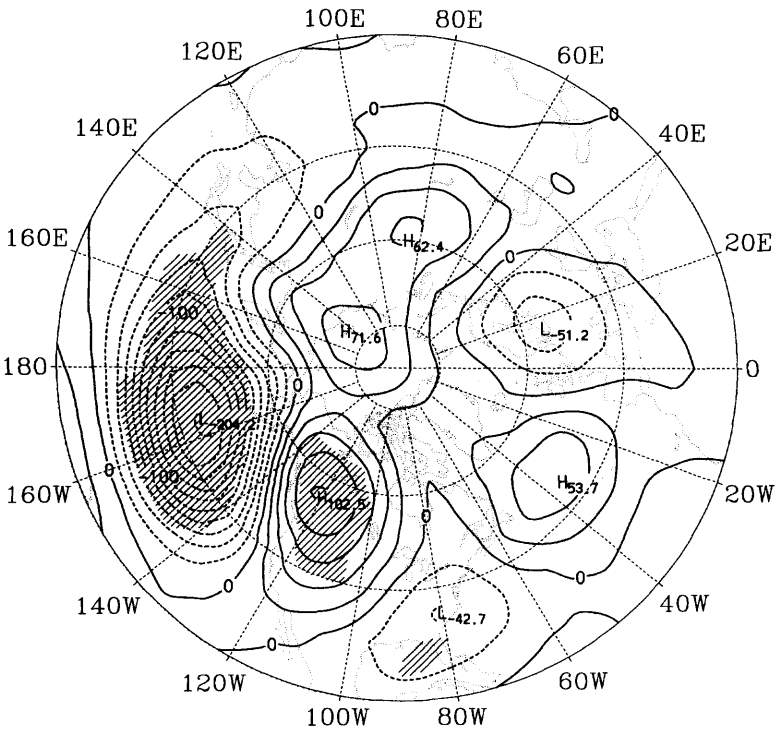


*Fig. 2.* Difference map obtained by subtracting the seasonal mean geopotential heights of winters with negative PNA from that with positive PNA at 500 hPa. The contour interval is 20 m. Dashed lines indicate negative values. Areas with significance levels greater than 99% are shaded.

in Fig. 3a. A belt of negative anomaly in the rms can be found along about 50°N across the North Pacific, and a belt of positive anomaly in the subtropical Pacific. This distribution indicates that during +PNA winters, the axis of the Pacific storm track is shifted southward from its position in −PNA winters. With the enhancement of the negative height anomaly over the North Pacific during the +PNA winters, a southward movement of the storm track is not surprising. The maximum positive centre near 150°W can be viewed as an indication of the eastward extension of storm track during positive PNA winters. This phenomenon was also observed by CV.

In the winter season the extratropical pressure and wind disturbances with periods longer than 10 days and shorter than a season normally occur with maximum intensity over the North Pacific and North Atlantic, and over northwest Siberia, near 80°E. Among other studies, the rms calculation by Blackmon et al. (1977) and the low-frequency eddy kinetic energy study by Sheng and Derome (1991) highlighted these features of the low-frequency flow. The centres of the low-frequency variance in the Pacific and Atlantic also correspond closely to the longitudes with the highest percentage of blocking flows, as determined by Rex (1950).

Fig. 3b shows the difference between the rms of the low-frequency 500 hPa geopotential height in +PNA and −PNA winters. The strength of the low-frequency variability is considerably reduced

*Fig. 3.* (a) Difference map obtained by subtracting the high-frequency transient height rms at 500 hPa of −PNA winters from that of +PNA winters; (b) As in (a), but for the low-frequency transient rms. The contour intervals are 5 m for (a) and 10 m for (b). Dashed lines indicate negative values. Areas with significance levels greater than 95% are shaded.

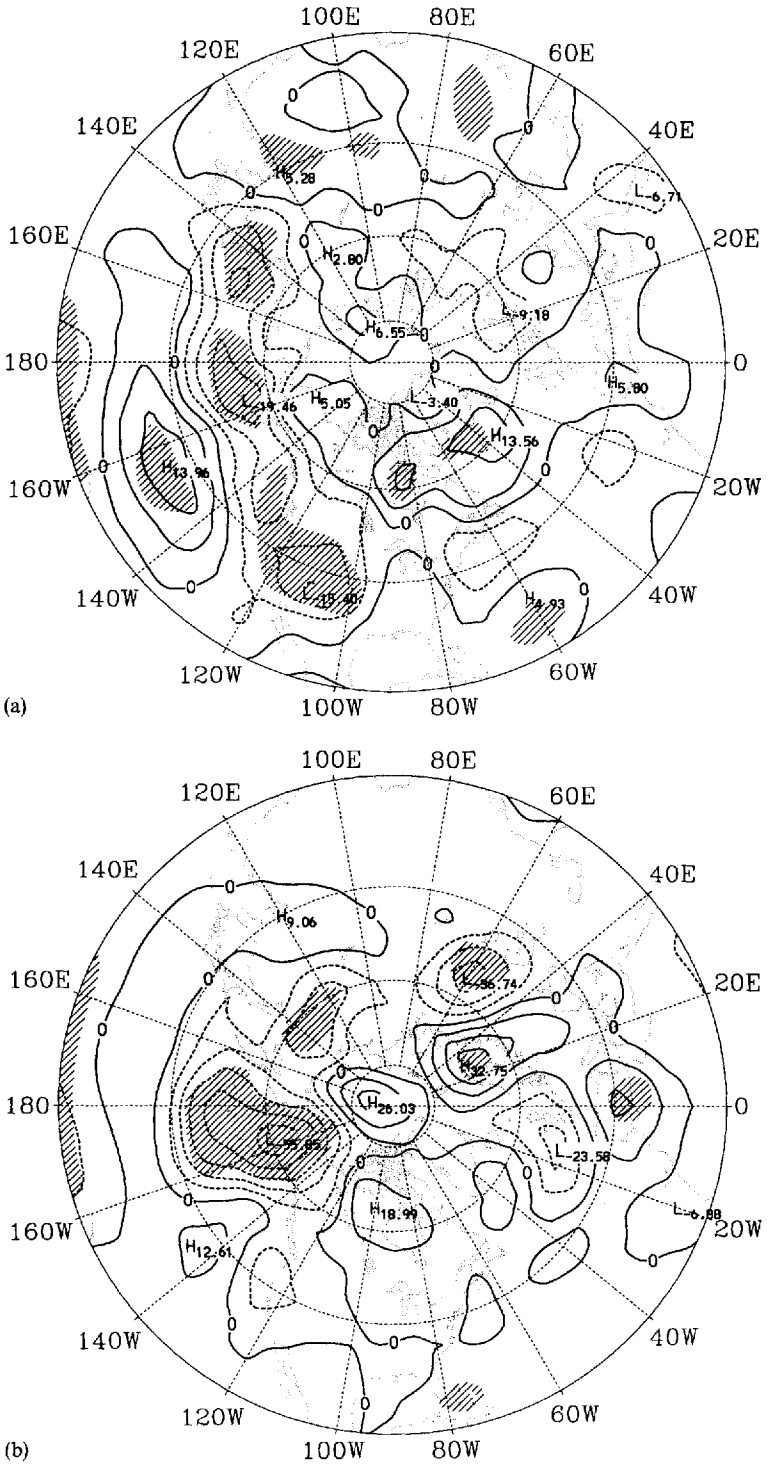
100E
80E
120E
60E
140E
40E
160E
20E
180
0
160W
20W
140W
40W
120W
60W
100W
80W
H 5.28
L -6.71
H 2.80
L -9.18
H 6.55
H 5.80
L -19.46
H 5.05
L -3.40
H 13.56
H 13.96
L -15.40
H 4.93
(a)
H 9.06
L -36.74
L -32.75
H 26.03
L -35.85
L -23.58
H 18.99
L -6.88
H 12.61
(b)

*Fig. 3.*

over the North Pacific during +PNA winters. The negative centre is collocated with the maximum rms centre over the North Pacific on the climatological map, in agreement with CV.

The distribution of the difference between the rms of the total transients in the 500 hPa geopotential height between the winters of positive and negative PNA anomalies (not shown) looks very similar to that of the low-frequency transients (Fig. 3b), implying that the reduction in the total transients in +PNA winters is mainly caused by the reduction in low-frequency variabilities.

Dole and Gordon (1983) studied the characteristics of the persistent anomalies of the wintertime Northern Hemisphere, where an anomaly was defined as the departure of the daily 500 hPa height from climatology. A persistent positive (negative) anomaly at a point was said to occur when the anomaly at that point remained equal to or greater (less) than a specified threshold value $M$ for at least $L$ days. As in Dole and Gordon (1983), we have calculated the number of persistent anomalies at each grid point with the threshold values of $M=+100$ m, $L=10$ days, and $M=-100$ m, $L=10$ days applied to the 500 hPa geopotential height. To remove possible effects of the brief transient fluctuations associated with the passing of synoptic-scale disturbances, the time series were first low-pass filtered. Fig. 4 shows the difference in the total number of the positive and negative persistent anomalies between winters of positive and negative PNA anomalies. The values shown have been normalized to numbers of cases per 10 years. The field has also been smoothed lightly by applying a 2-dimensional 9-point spatial filter as used by Dole and Gordon (1983) for display purposes. Consistent with Fig. 3b, a reduction in the number of persistent anomalies can be found in the North Pacific region during +PNA winters.

We have also calculated the differences between +PNA and −PNA winters in the numbers of

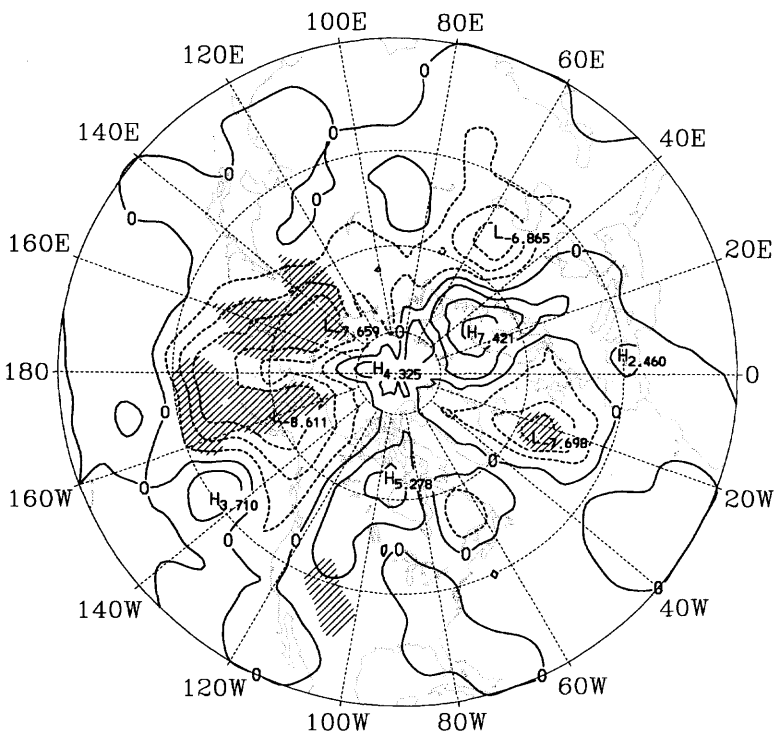


*Fig. 4.* Difference map obtained by subtracting the total number of positive and negative persistent anomalies in the −PNA winters from that of +PNA winters. Values have been normalized to numbers per 10 years. The contour interval is 2 and contours with negative values are dashed.

positive and negative persistent anomalies separately (figures not shown). Their patterns are similar to Fig. 4, so that the numbers of both positive persistent anomalies and negative persistent anomalies decrease during +PNA winters. The number of blocking events over the North Pacific is thus likely to be smaller when the background flow shows a +PNA anomaly.

## 4. Interactions between the low-frequency and other time scales

We have seen that there is a significant reduction of the low-frequency eddy activity in the North Pacific during winters with a mean-seasonal positive PNA anomaly. To shed some light on this observation, we turn to a study of the interactions among three frequency bands: the low-frequency transients, the high-frequency transients and the background seasonal mean flow.

To study the contributions to the low-frequency height variance from different sources, we use the budget equation for the low-frequency variance. From the barotropic vorticity equation and with the geostrophic approximation, the geopotential height tendency of the low-frequency variation can be expressed as:

$$\frac{\partial z_1}{\partial t} = A_1 + B_1 + C_1 + D_1 , \tag{2}$$

where $D_l$ includes all the subgrid dissipative effects, and

$$A_1 = -\frac{f}{g}\nabla^{-2}[\bar{V}\cdot\nabla\zeta_1 + V_1\cdot\nabla(\bar{\zeta}+f)] - \frac{f}{g}\nabla^{-2}[(f+\bar{\zeta})\nabla\cdot V_1 + \zeta_1\nabla\cdot\bar{V},$$

$$B_1 = -\frac{f}{g}\nabla^{-2}\nabla\cdot(V_1\zeta_1)_1 ,$$

$$C_1 = -\frac{f}{g}\nabla^{-2}\nabla\cdot(V_h\zeta_h)_1 - \frac{f}{g}\nabla^{-2}\nabla\cdot(V_h\zeta_1 + V_1\zeta_h)_1 .$$

$\zeta$ is the relative vorticity, $V$ is the horizontal velocity vector. The overbar represents the seasonal mean, and the subscripts l and h refer to the low- and high-frequency filtered data, respectively.

Term $A_1$ represents the interaction between the low-frequency flow and the time-averaged flow; term $B_1$ is the contribution from the low-frequency flow itself; term $C_1$ represents the interaction between the low- and high-frequency transients. As discussed by Sheng and Derome (1993), the second term in $C_1$ is relatively small compared to its first term, so that $C_1$ is dominated by the vorticity flux convergence by the high-frequency eddies.

We are here interested in the vertical integration of each term in (2), i.e., the barotropic effects. Considering that the wind data are available only at 250 and 850 hPa, we will use the average of each term at these two levels to represent the column average. So in the following discussion in this section, the geopotential height $z_1$ and each term on the right-hand-side of (2) refer to the average of those at 250 and 850 hPa.

By multiplying (2) with $z_1$, the two-level averaged low-frequency component of geopotential height, and then averaging over time, we obtain the covariance of the low-frequency geopotential height and the height tendency, or the tendency of the low-frequency height variance:

$$\frac{\partial}{\partial t}\left(\frac{1}{2}\overline{z_1^2}\right) = \overline{z_1 A_1} + \overline{z_1 B_1} + \overline{z_1 C_1} + \overline{z_1 D_1} . \tag{3}$$

### 4.1. *Interaction with the mean flow*

To see the difference in the contribution to the covariance from the mean flow between winters with positive and negative PNA anomalies, a comparison is made between the composites of $\overline{z_1 A_1}$ for these two conditions. Fig. 5 shows the distribution of $\overline{z_1 A_1}$ for the +PNA and −PNA winters, and their difference. For the −PNA winters, a large area with positive values is found over the North Pacific (middle panel), indicating that the low-frequency fluctuations owe some of their variance to their interactions with the seasonal mean flow. In the case of the +PNA winters, the positive values of covariance in this region are reduced (upper panel). From Fig. 5c, obtaining by subtracting Fig. 5b from Fig. 5a, it is clear that in the North Pacific there is a notable reduction in the contribution from the background mean flow when there is a positive PNA anomaly.

From the definition of $A_1$, it can be seen that the contribution to the low-frequency height variance from the interaction with the seasonal mean flow can be separated into two terms: the contribu-

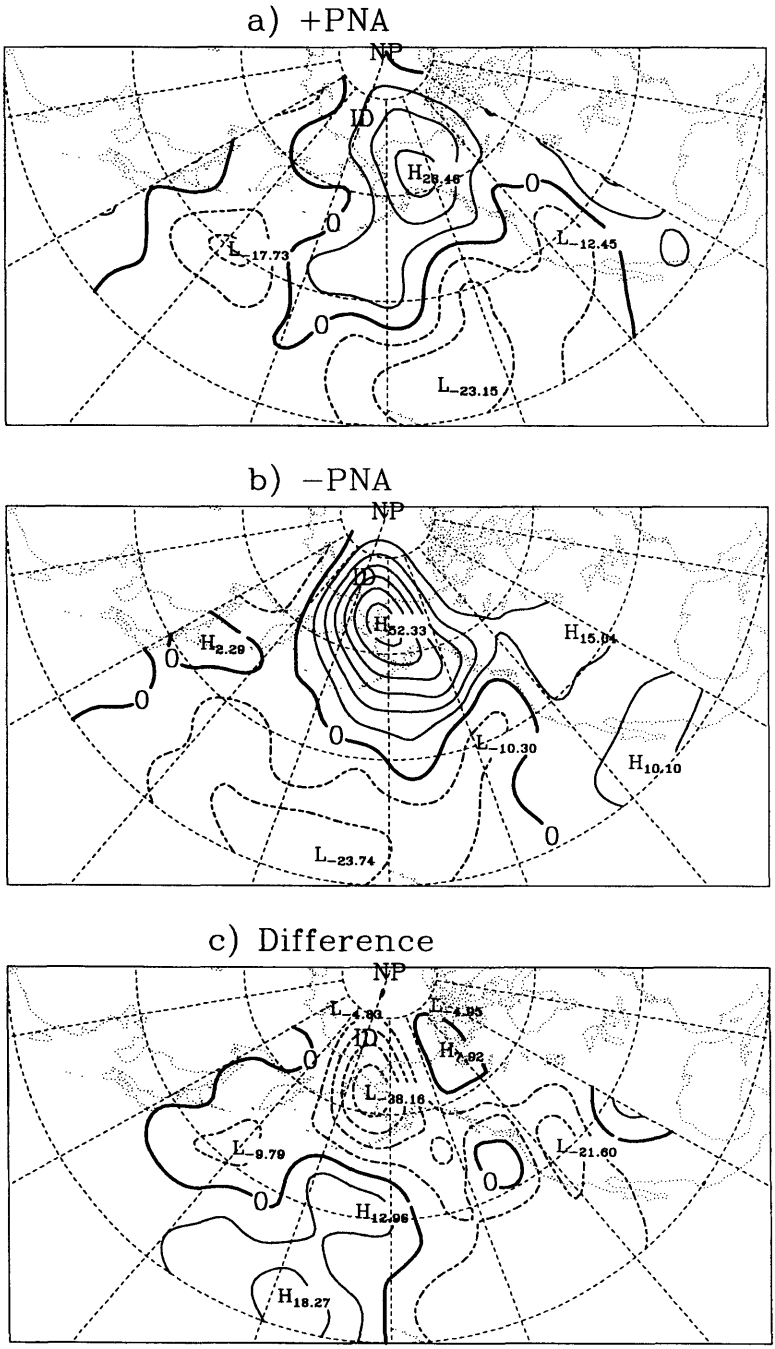


*Fig. 5.* Low-frequency height variance tendency caused by the interaction with the mean flow for: (a) +PNA winters; (b) −PNA winters; and (c) the net difference between +PNA and −PNA winters. The contour intervals are $8 \times 10^{-3}$ m$^2$/s.

tion from vorticity advection and that from divergence. As a vertical average is used in this study, the contribution from the divergence should be largely canceled out, and is found to be one order smaller than the effect of the vorticity advection. Hence the low-frequency height variance from the seasonal mean flow is dominated by the contribution from the vorticity advection.

### 4.2. *Interaction with the high-frequency eddies*

The low-frequency height variance tendency caused by the interactions with the high-frequency transients is represented by $\overline{z_l C_l}$. Its geographic distribution for the +PNA and −PNA winters and their difference are presented in Fig. 6. During −PNA winters (middle panel), the covariance between $z_l$ and the high-frequency transient forcing is positive throughout the extratropical Pacific, with a centre near 160°W and 60°N, indicating that the vorticity flux convergence by the high-frequency eddies is forcing the low-frequency geopotential height variations in the North Pacific.

In the +PNA winters (upper panel of Fig. 6), the positive covariance between the low-frequency geopotential height and the barotropic high-frequency eddy forcing is limited to the eastern Pacific, with a much smaller area than its counterpart in the −PNA winters. The contribution of the high-frequency transients to the low-frequency eddies over the northwest Pacific is seen to be largely reduced. In the the difference map (Fig. 6c), negative values dominate over the North Pacific, and their magnitudes are about one third of that caused by the seasonal mean flow (Fig. 5c).

The high-frequency transient eddies affect the slowly-varying flow not only through their vorticity flux, but also through their heat flux. Holopainen (1994) showed that in the upper troposphere the forcing of the geopotential height associated with the eddy heat flux is opposite to that due to the eddy vorticity flux. As a result, the total net forcing in the upper troposphere is much weaker than that estimated from the two-dimensional (barotropic) version of the tendency method. The relative effects of the thermal and vorticity fluxes can be seen from the longitude-pressure distributions of zonal wind tendencies along 40°N, shown in Fig. 4 of Lau and Holopainen (1984). The forcing by the heat flux changes sign from the upper to the lower troposphere, causing a westward acceleration of the time-mean flow in the upper troposphere and eastward acceleration in the lower troposphere in the storm track longitudes. The forcing by vorticity transports has the same sign at all the levels with strong eastward acceleration of the time-mean flow in the upper troposphere in the storm track longitudes.

The thermal effect should be largely canceled out in the vertical integration of the total net forcing throughout the troposphere. Left in the vertical integral is mostly the forcing due to the eddy vorticity transports. Hence, the vertical average of the forcing due to the eddy vorticity transports in this study should give an adequate representation of the mid-tropospheric forcing by the transient eddies.

## 5. The feedback of the high- and low-frequency transients onto the seasonal mean flow

We have seen significant differences between the +PNA and −PNA winters in the low-frequency eddies and the synoptic-scale transients. In this section we will investigate the feedback effect due to the modified low- and high-frequency eddies.

The geopotential height tendency of the time-mean motion can be written as:

$$\frac{\partial \bar{z}}{\partial t} = -\frac{f}{g}\nabla^{-2}[\nabla\cdot(\overline{\zeta_h V_h})] - \frac{f}{g}\nabla^{-2}[\nabla\cdot(\overline{\zeta_l V_l})] + \frac{f}{g}\nabla^{-2}\bar{\mathscr{R}}. \quad (4)$$

This equation is similar to (2) except that the tendency is for the time-averaged geopotential here while in (2) the tendency was projected onto the low-frequency. $\bar{\mathscr{R}}$ refers to all remaining components in the vorticity equation, such as the horizontal advection by the time mean flow, and friction. As previously, the geopotential height $z$ and the eddy forcing refer to the average of those at 250 and 850 hPa. In the following we will refer to the first and second terms on the right-hand-side of (4) as the forcing by the high- and low-frequency eddies, respectively.

Fig. 7a is the difference in the geopotential height tendency caused by the high-frequency eddies between +PNA and −PNA winters, which is obtained by subtracting composite of the high-

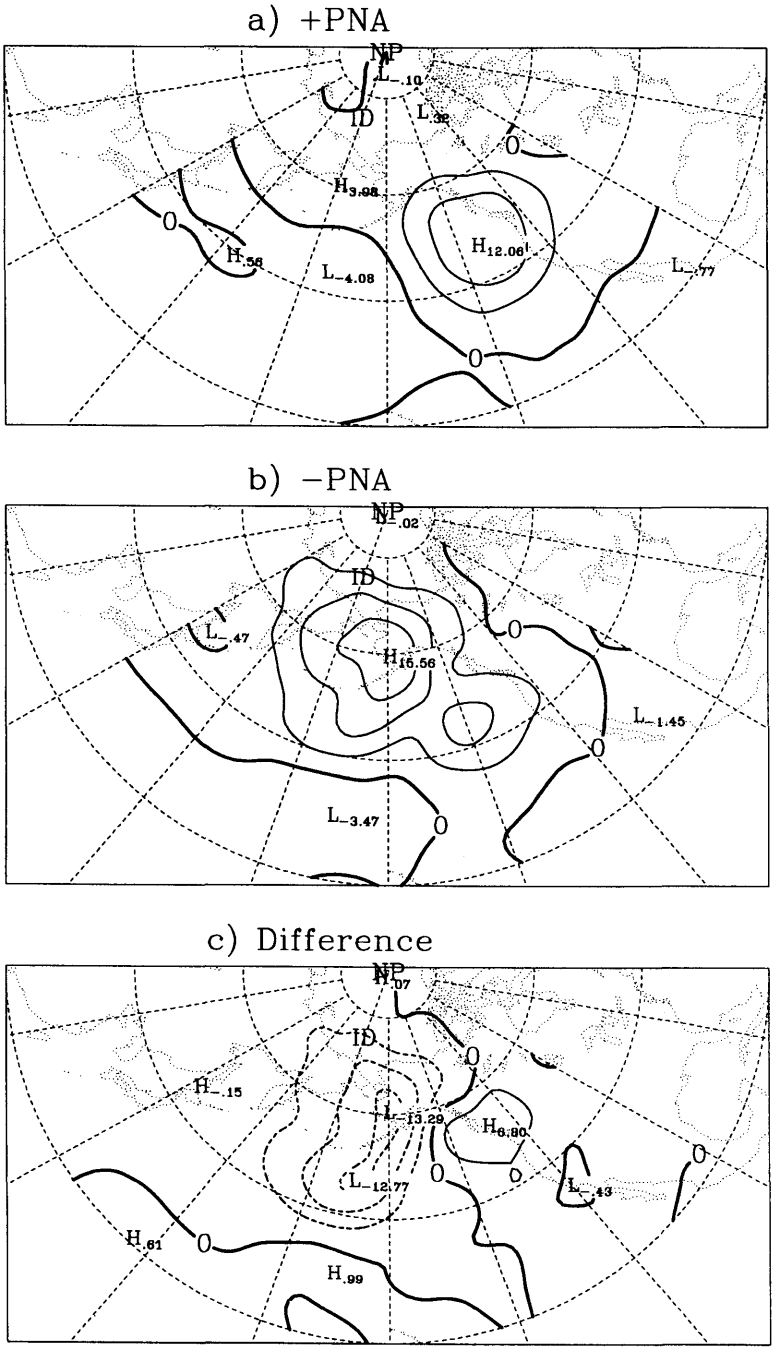


*Fig. 6.* Covariance between low-frequency geopotential height and the synoptic-scale eddy forcing: (a) +PNA winters; (b) −PNA winters; and (c) the net difference between +PNA and −PNA winters. The contour intervals are $4 \times 10^{-3}$ m$^2$/s.

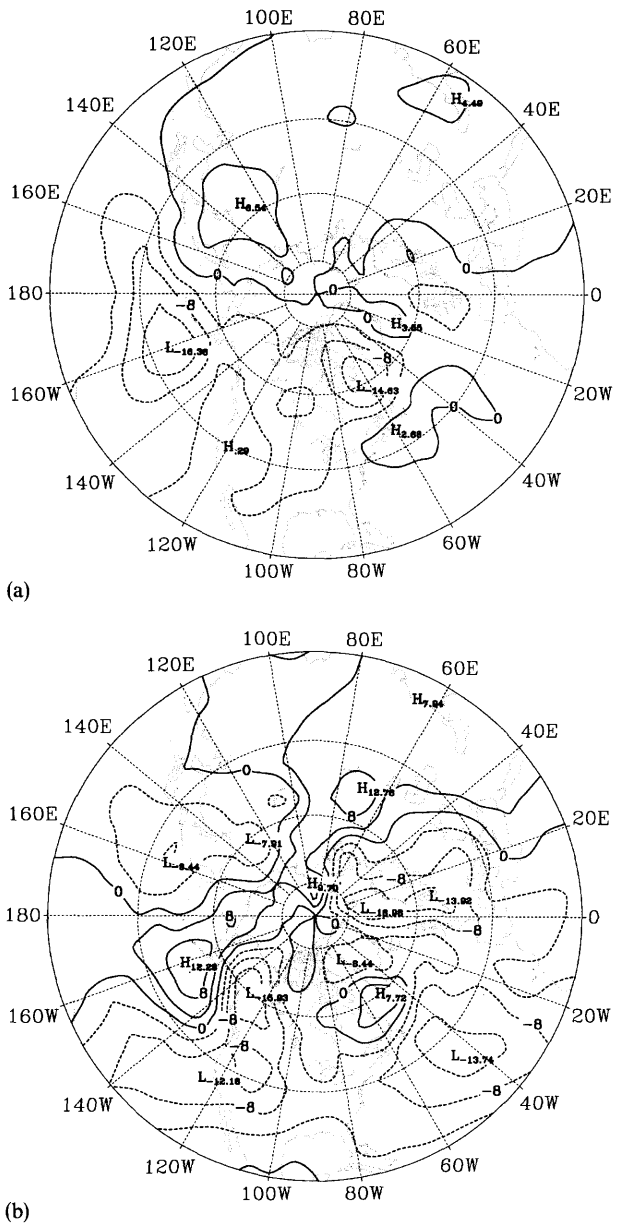


*Fig. 7.* Difference map as obtained by subtracting the seasonal mean geopotential height tendency caused by (a) high-frequency eddies; (b) low-frequency eddies in −PNA winters from that in +PNA winters. The contour intervals are $4 \times 10^{-5}$ m/s.

frequency eddy forcing in −PNA winters from that in +PNA winters. We see that there is an anomalous negative height forcing pattern over the North Pacific, coinciding with the seasonal-mean negative height anomaly presented in Fig. 2. During +PNA winters the eastward extension of the synoptic-scale baroclinic waves produces a barotropic forcing that tends to deepen the

Aleutian low, and accelerates the seasonal mean zonal flow to the south. Thus the vorticity flux convergence by the high-frequency transients is reinforcing and maintaining the seasonal-mean height anomaly. The role of the synoptic-scale transients in maintaining the height anomaly has been reported in some previous studies. By studying the synoptic-scale transient forcing of the monthly PNA pattern, Klasa et al. (1992) found that the eddy barotropic forcing is in phase with the height anomaly. Kok and Opsteegh (1985) and Ting and Hoerling (1993) showed that the extratropical wave train anomalies during the 1982/83 and 1986/87 El Niño winters were maintained by the transient eddy forcing.

The feedback of the intraseasonal low-frequency variabilities onto the seasonal mean flow is different from that of the synoptic-scale eddies. Fig. 7b shows the difference of the geopotential height tendency caused by the low-frequency eddies between the +PNA and −PNA years. An area of positive values covers the North Pacific. This pattern tends to be out of phase with the PNA anomalies, suggesting that the low-frequency transients act to dissipate the large-scale seasonal-mean wave anomaly pattern.

## 6. Summary and discussion

We have analyzed the differences between the winters with positive and negative PNA patterns. Significant differences have been found in the winter seasonal mean flow and transient activities. Special attention has been paid to the difference in the extratropical low-frequency variabilities and the mechanisms supporting them.

During the winters with a positive PNA anomaly in the seasonal mean flow, the most striking feature is the deepening of the Aleutian low over the North Pacific, and the eastward extension of the subtropical Pacific westerly jet. We have shown that this is accompanied by a reduced low-frequency eddy activity in the North Pacific, and by less frequent persistent, large-amplitude anomalies in this area. The high-frequency baroclinic wave activity is shifted southward along the extended westerly jet.

The mechanisms associated with the decrease of the low-frequency transient activity over the North Pacific during +PNA winters are analyzed by means of the low-frequency height variance tendency equation. When there is a positive PNA anomaly in the seasonal mean flow, the modified interaction between the seasonal mean flow and the low-frequency transients leads to a smaller generation of the low-frequency variance. Also, the strong seasonal mean Aleutian low tends to keep the baroclinic synoptic-scale eddies moving along its southern side, leading to only weak interactions between the high- and low-frequency eddies over the northern Pacific and thus to less synoptic-scale eddy forcing of the low-frequency flow in that region.

Since the intraseasonal eddy activity varies from a positive PNA to a negative PNA basic mean flow, we would expect medium and extended range forecast errors to grow differently in these two distinct weather regimes. This conjecture is supported by Lin and Derome (1996) who performed a large number of forecast experiments using a T21 3-level quasi-geostrophic model. They found that after about one week the forecast error grows faster when the forecasts are made during a negative PNA regime than during a positive one. This was particularly noticeable over the North Pacific, the North American and North Atlantic regions.

It should be kept in mind that the results presented in this study are based on data which cover a period of only two decades and have relatively coarse horizontal resolution. Only 7 +PNA winters are composited for comparison with 8 −PNA winters. Some degree of caution is needed in interpreting the results. Variability exists from case to case even in the same group. Some features in the composite for either the +PNA or the −PNA regimes may be biased toward the stronger ones in that group. Some calculations such as the tendency of the low-frequency variance may be sensitive to the horizontal resolution, but their large-scale features described in this study should remain qualitatively unchanged.

## 7. Acknowledgements

This research was supported by grants from the Natural Sciences and Engineering Research Council and the Atmospheric Environment Service of Canada.

## REFERENCES


Blackmon, M. L., Wallace, J. M., Lau, N. C. and Mullen, S. L. 1977. An observational study of the Northern Hemisphere wintertime circulation. *J. Atmos. Sci.* **34**, 1040–1053.

Branstator, G., Mai, A. and Baumhefner, D. P. 1993. Identification of highly predictable flow elements for spatial filtering of medium- and extended-range numerical forecasts. *Mon. Wea. Rev.* **121**, 1786–1802.

Chen, W. and Van Den Dool, H. M. 1995. Low-frequency variabilities for widely different basic flows. *Tellus* **47A**, 526–540.

Dole, R. M. and Gordon, N. D. 1983. Persistent anomalies of the extratropical Northern hemisphere wintertime circulation: Geographical distribution and regional persistence characteristics. *Mon. Wea. Rev.* **111**, 1567–1586.

Holopainen, E. O. 1994. Cyclone climatology and its relationship to planetary waves and physiography. In: *Proceedings of an International Symposium on the Life cycles of extratropical cyclones, vol. I* (eds. S. Grønås and M. Shapiro). Bergen-Norway, pp. 72–79.

Hoskins, B. J., James, I. N. and White, G. H. 1983. The shape, propagation and mean-flow interaction of large scale weather systems. *J. Atmos. Sci.* **40**, 1595–1612.

Kok, C. J. and Opsteegh, J. D. 1985. On the possible causes of anomalies in seasonal mean circulation pattern during the 1982–83 El Nino event. *J. Atmos. Sci.* **42**, 677–694.

Klasa, M., Derome, J. and Sheng, J. 1992. On the interaction between the synoptic-scale eddies and the PNA teleconnection pattern. *Beitr. Phys. Atmosph./Contrib. Atmos. Phys.* **65**, 211–222.

Lau, N.-C. 1988. Variability of the observed midlatitude storm tracks in relation to low-frequency changes in the circulation pattern. *J. Atmos. Sci.* **45**, 2718–2743.

Lau, N.-C. and Holopainen, E. O. 1984. Transient eddy forcing of the time-mean flow as identified by geopotential tendencies. *J. Atmos. Sci.* **41**, 313–328.

Lin, H. and Derome, J. 1996. Changes in predictability associated with the PNA pattern. *Tellus* **48**, in press.

Mansfield, D. A. 1986. The skill of dynamical long-range forecasts, including the effect of sea surface temperature anomalies. *Q. J. R. Meteorol. Soc.* **112**, 1145–1176.

Miyakoda, K., Sirutis, J. and Ploshay, J. 1986. One month forecast experiments—without anomaly boundary forcing. *Mon. Wea. Rev.* **114**, 2363–2401.

Palmer, T. N. 1988. Medium and extended range predictability and stability of the Pacific/North American mode. *Q. J. R. Meteorol. Soc.*,**114**, 691–713.

Renwick, J. A. and Wallace, J. M. 1995. Predictable anomaly patterns and the forecast skill of Northern Hemisphere wintertime 500-mb height fields. *Mon. Wea. Rev.* **123**, 2114–2131.

Rex, D. F. 1950. Blocking action in the middle troposphere and its effect upon regional climate (II). The climatology of blocking action. *Tellus* **2**, 275–301.

Sheng, J. and Derome, J. 1991. An observational study of the energy transfer between the seasonal mean flow and transient eddies. *Tellus* **43A**, 128–144.

Sheng, J. and Derome, J. 1993. The dynamic forcing of the slow transients by the synoptic-scale eddies: An observational study. *J. Atmos. Sci.* **50**, 757–771.

Ting, M.-F. and Hoerling, M. P. 1993. The dynamics of stationary wave anomalies during the 1986/87 El Niño. *Climate Dynamics* **9**, 147–164.

Wallace, J. M., Zhang, Y. and Lau, K.-H. 1993. Structure and seasonality of interannual and interdecadal variability of the geopotential height and temperature fields in the Northern Hemisphere troposphere. *J. Climate* **6**, 2063–2082.